Food Chemistry: X 22 (2024) 101366

Contents lists available at ScienceDirect

Food Chemistry: X

journal homepage: www.sciencedirect.com/journal/food-chemistry-x

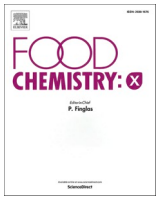

Effect of mitochondrial calcium homeostasis-mediated endogenous enzyme activation on tenderness of beef muscle based on MCU modulators

Zhenjiang Ding [b,1], Chunmei Liu [a,1], Zihan Zhang [a], Chunhui Zhang [a], Feng Huang [a,c,*]

[a] Institute of Food Science and Technology, Chinese Academy of Agricultural Sciences/Key Laboratory of Agro-Products Processing, Ministry of Agriculture and Rural Affairs, Beijing 100193, China
[b] Beijing Key Laboratory of the Innovative Development of Functional Staple and Nutritional Intervention for Chronic Diseases, China National Research Institute of Food and Fermentation Industries, Beijing 100015, China
[c] Western Agricultural Research Center, Chinese Academy of Agricultural Sciences, Changji 831100, China

ARTICLE INFO

Keywords:
Mitochondrial calcium homeostasis
Mitochondrial dysfunction
Oxidative stress
Endogenous enzyme
Tenderness

ABSTRACT

The mitochondrial calcium uniporter (MCU) occupies a noteworthy position in the regulation of mitochondrial calcium uptake. This study investigated the effects of MCU modulator-mediated mitochondrial calcium on mitochondrial dysfunction, oxidative stress, endogenous enzyme activities, and tenderness during postmortem aging. Spermine, as an activator of MCU, resulted in an increase in mitochondrial calcium levels, not only disrupting mitochondrial morphology but also triggering mitochondrial oxidative stress and downregulation of antioxidant factors. Additionally, the spermine group underwent later activation of calpain and earlier activation of caspases, as well as the myofibril fragmentation index was initially lower and then higher compared with control group, indicating that endogenous enzymes played an indispensable role in different aging periods. Interestingly, the results of the Ru360 (an inhibitor of MCU) group were opposite to those aforementioned findings. Our data provide a novel perspective on the regulatory mechanism of mitochondrial calcium homeostasis mediated by MCU on tenderness.

1. Introduction

It has been proposed that apoptosis is one of the key molecular mechanisms controlling postmortem (PM) tenderization (Wang et al., 2018). At present, there are three main apoptotic pathways: the first is the caspase-8- and caspase-10-mediated exogenous death receptor signaling pathways. Second, the cytochrome *c* release and the caspase-3 activation-related intrinsic mitochondrial signaling pathway. Third, the caspase-12-regulated endoplasmic reticulum signaling pathway (Zou, Yu, Shao, Sun, & Li, 2022). Previous studies have suggested that the mitochondrial pathway may be necessary for oxidative stress-mediated apoptosis to occur during PM aging (Wang et al., 2018). Analogously, mitochondria-induced apoptosis is primarily due to mitochondrial dysfunction and redox homeostasis imbalance (Ma, Zhang, Wang, Yu, & Han, 2023). The primary organelle that produces reactive oxygen species (ROS) is the mitochondria, which is also the organelle that is most frequently targeted for attack (Ding, Wei, Liu, Zhang, & Huang, 2022). ROS generated by single electron transfer could result in mitochondrial membrane swelling or loss of membrane potential after animal bleeding (Liu et al., 2023; Zhang, Ma, & Kim, 2020). Cytochrome c is released from the mitochondria to the cytoplasm to bind Apaf-1, dATP/ATP and pro-caspase-9 when mitochondrial permeability increases, triggering executioner caspase activation (Green, 2005).

Numerous reports have stated that Ca^{2+} levels are crucial for regulating the tenderness of meat (Cao et al., 2012; Wang, Han, Ma, Yu, & Zhao, 2017). PSE (pale, soft and exudative) meat had a higher apoptotic potential than RFN (reddish-pink, firm and nonexudative) meat at 1 h PM, which may be related to Ca^{2+} channel disorder (Guo et al., 2016). Kiyimba et al. (2022) clarified that differential proteins between dark-cut and normal-pH beef played an important role in regulating cellular Ca^{2+} homeostasis using LC–MS/MS-based proteomics. The increase in cytoplasmic Ca^{2+} levels could accelerate muscle acidification by activating sarcoplasmic reticulum calcium ATPase, leading to a surging rate of ATP hydrolysis (Scheffler & Gerrard, 2007). Additionally, Ca^{2+} accelerated the rate of glycolysis, thereby promoting H^{+} accumulation and pH reduction, mediating PM tenderization (Zou, Jia, Ji, Li, &

* Corresponding author at: No.1, Nongda South Rd., Xi Beiwang, Haidian District, Beijing 100193, China.
E-mail address: fhuang226@163.com (F. Huang).
[1] Both authors contributed equally to the work.

https://doi.org/10.1016/j.fochx.2024.101366
Received 25 January 2024; Received in revised form 24 March 2024; Accepted 5 April 2024
Available online 7 April 2024

Dai, 2023). Moreover, calpain is a well-known Ca^{2+}-dependent cysteine protease that can promote the transfer of cytochrome *c* by mediating the cleavage of Bcl-2 family members, and hydrolyzing myofibrillar proteins (Ding, Wei, Zhang, Zhang, & Huang, 2021; Jia et al., 2021). Mitochondria, as key regulators of cytoplasmic free Ca^{2+}, are closely related to cell metabolism and cell survival in their uptake of Ca^{2+} (Zou et al., 2023). The mitochondrial calcium uniporter (MCU), which is present in the inner membrane of mitochondria, controls the release of Ca^{2+} from the cytoplasm into the mitochondria. Dang et al. (2020) found that MCU expression in very tender steaks was lower than that in intermediate tender steaks. Nevertheless, the mechanism of endogenous enzyme activities and tenderization mediated by MCU remains unclear. Intriguingly, the upregulation of MCU in colorectal cancer led to an increase in mitochondrial Ca^{2+} uptake, which further enhanced mitochondrial ROS production by promoting mitochondrial biogenesis (Liu et al., 2020). We hypothesized that MCU could affect mitochondrial functional integrity and redox balance by governing mitochondrial Ca^{2+} intake and ultimately regulate apoptosis pathway-mediated meat tenderization. Therefore, we injected spermine/Ru360 into the *Longissimus thoracic* (LT) muscle of PM cattle, which is a specific activator/inhibitor of MCU. The aim was to clarify the regulatory mechanism of MCU on tenderness by evaluating the changes in mitochondrial Ca^{2+} levels after MCU activation or inhibition, as well as its impact on the acceleration or delay of mitochondrial dysfunction and oxidative stress during PM aging.

2. Materials and methods

2.1. Muscle sampling

Six Chinese yellow cattle with similar genetic backgrounds were fed and managed under the same conditions at Dachang Farm, Hebei Province, China. Following the guidelines of the Chinese Academy of Agricultural Sciences' Animal Care and Ethics Committee (ID: IAS20160616), all cattle (606 ± 15 kg body weight) were slaughtered at Hebei Fucheng Wufeng Food Co. LTD, a commercial meat processing company. Within 20 min of exsanguination, LT muscles were separated into 18 equal-size sections (2 cm × 2 cm × 2 cm, three groups × six aging periods) per carcass, and 108 slices were obtained from six cattle for six replications. The first group was injected with physiological saline at a ratio of 1:1 (*w/v*) (meat/buffer) as the control group. The second group was injected with the same proportion of spermine (an MCU activator, 20 μmol/L) as the spermine group. The third group was injected with Ru360 (an MCU inhibitor, 20 μmol/L) as the Ru360 group. All samples were obtained at 4 °C for 0, 6, 12, 24, 72, and 120 h PM, immediately prepared for electron microscopy and then instantly frozen in liquid nitrogen for biochemical analysis.

2.2. Mitochondrial isolation

Mitochondria were isolated as previously reported with minor modifications (Zhang et al., 2020). The meat samples were homogenized for 1 min at 10000 g using precooled extraction buffer. After centrifuging the homogenate twice for 10 min at 1000 *g*, the resulting supernatant was centrifuged for 10 min at 8000 *g*, and the precipitate was then resuspended in the extraction buffer. A BCA Protein Assay Kit was used to measure the protein content.

2.3. Determination of Ca^{2+} concentration in mitochondria

A mitochondrial Ca^{2+} concentration fluorescence detection kit (Genmed Scientifics INC, USA) was used to measure the changes in mitochondrial Ca^{2+} uptake during PM aging after treatment with MCU modulators. After adjusting the mitochondrial protein concentration to 1 mg/mL, the staining solution was incubated. The intensity of the fluorescence was measured using a Synergy™ H1 microplate reader, with excitation and emission wavelengths of 550 and 590 nm, respectively.

2.4. Determination of mitochondrial permeability transition pore (MPTP) opening

A few minor adjustments were made to the protocol to follow Wang et al. (2017). With the opening of the MPTP, the permeability of the mitochondrial inner membrane to sucrose and mannitol was enhanced, as manifested by a decrease in absorbance at 540 nm. The mitochondrial suspension was incubated with three volumes of MPTP detection buffer (pH 7.4) containing 230 mM mannitol, 70 mM sucrose, and 3.0 mM Hepes. A UV spectrophotometer was used to detect the absorbance at 540 nm.

2.5. Mitochondrial micromorphology detection

Ultrastructural observation was performed by the method of Wang et al. (2021). A 1 mm × 1 mm × 1 mm incision was made from the muscle samples before freezing in liquid nitrogen. The samples were fixed in a 2.5% glutaraldehyde solution, and then fixed with 1% osmium tetroxide after rinsing with phosphate buffer, followed by ethanol gradient dehydration. Subsequently, specimens were embedded with Epon812 resin and sectioned with Power TOM-XL. Finally, utilizing a transmission electron microscope (Hitachi H-750, Japan), mitochondrial micromorphology was acquired after the ultrathin slices were stained.

2.6. Determination of mitochondrial ROS and antioxidant capacity

The degree of oxidative stress of mitochondria and total antioxidant capacity were assessed. 2′,7′-Dichlorohydrofluorescein diacetate (DCFH-DA), a nonfluorescent dye that can penetrate cells, can be deacetylated by cellular esterases to nonfluorescent DCFH, which quickly converts to DCF with high fluorescence when reacting with ROS. Therefore, after 0.5 h of treatment with DCFH-DA (10 μM) at 37 °C, the fluorescence of the mitochondrial suspension was measured at 480/525 nm (the wavelength of excitation and emission). The water-soluble formazan dye may be produced by WST-1 reacting with the superoxide anion (O^{2-}) that xanthine oxidase generates, and superoxide dismutase (SOD) could undergo a disproportionation reaction with O^{2-}, reducing the generation of formazan dye. Reduced glutathione (GSH) could react with DTNB to generate TNB (a yellow compound) with absorbance at 405 nm. In brief, the muscle samples were homogenized in phosphate buffer (pH 7.2) containing 2% sodium dodecyl sulfate (SDS) to obtain the total protein extraction solution. The level of mitochondrial ROS, as well as the SOD activity and GSH content, which characterize antioxidant capacity, were detected in accordance with Nanjing Jiancheng Bioengineering Institute (Nanjing, China) appropriate kits.

2.7. Determination of calpain activity

The sarcoplasmic proteins were obtained following our published work (Ding et al., 2021). For three 10 s bursts at a speed of 15,000 g, the samples were homogenized using cold lysis buffer, and the supernatant after centrifugation was sarcoplasmic proteins. Reaction buffer and substrate from a calpain activity test kit (93-K240–100, Biovision, USA) were treated with sarcoplasmic proteins. The fluorescence was measured at 400/505 nm (the wavelength of excitation and emission).

2.8. Determination of caspase activities

Referring to the method of Ding et al. (2021), sarcoplasmic proteins were incubated with reaction buffer and LEHD-AFC/DEVD-AFC (substrates of caspase-9 and caspase-3, respectively) from caspase activity assay kits (K118/K533, Biovision, USA). The fluorescence was measured at 400/505 nm (excitation wavelength/emission wavelength).

2.9. Determination of myofibril fragmentation index (MFI)

The MFI was carried out in compliance with the protocols outlined by Olson, Parrish, and Stromer (1976) and modified by Wang et al. (2022). The sample was homogenized and centrifuged with 10 times the volume of pre-cooled buffer solution (1 mM $MgCl_2$, 1 mM EDTA, 20 mM K_2HPO_4, 100 mM KCl, and pH 7.0), and the operation was repeated twice. The precipitate was resuspended with the same volume of buffer solution and protein concentration was adjusted to 0.5 mg/mL. The MFI value was calculated as the absorbance (540 nm) multiplied by 200.

2.10. SDS–PAGE and western blotting

After extracting all of the proteins, the protein concentration was determined. Soaking treatment buffer was added to the SDS–PAGE samples. A 4% stacking gel and a 12.5% separating gel were used to determine the expression level of MCU. The gels were run at constant 80 V and 120 V for 30 min and 90 min, respectively. Polyvinylidene fluoride membranes were immediately filled with the gel contents and left at 4 °C for 90 min at 200 mA. The membrane was then incubated with anti-MCU (ab110325, Abcam) and anti-GAPDH (ab8245, Abcam) overnight after blocking with TBST buffer containing 5% skim milk powder for 2 h. The membrane was rinsed with TBST four times for ten minutes, both before and after incubation with HRP-conjugated goat anti-rabbit IgG. The band image was captured using a ChemiDoc TMMP Imaging System (Bio-Rad, CA, USA), and Quantity One software (Bio-Rad, CA, USA) handled the grayscale level analysis.

2.11. Statistical analysis

Utilizing SPSS 25.0 software, the Analysis of Variance (ANOVA) was performed on all data, along with the New Multiple-range test of Duncan and LSD. Treatments, aging time and their interaction were used as fixed effects, and animals were considered random effects. The results are presented as the mean ± SE. P values <0.05 were considered statistically significant.

3. Results and discussion

In this study, we utilized spermine/Ru360 to evaluate the mechanism of MCU-mediated mitochondrial calcium homeostasis on meat tenderness. Spermine, as an MCU activator, promoted the entry of cytosolic Ca^{2+} into mitochondria (Qiu et al., 2020). In contrast, Ru360 is an MCU-specific inhibitor with significant inhibitory effect on mitochondrial Ca^{2+} uptake (Sun et al., 2023). Sustained Ca^{2+} transfer could lead to mitochondrial dysfunction. The redox balance of mitochondria regulated by MCU is essential for the normal respiration and mobility of mitochondria (Weiser et al., 2023). Calpain and caspases, as key endogenous enzymes for hydrolyzing myofibrillar proteins and improving tenderness in PM muscles, could be activated by calcium ions and the intrinsic mitochondrial signaling pathway, respectively (Huang et al., 2014; Huang, Huang, Zhou, Xu, & Xue, 2011). As a consequence, we chose prerigor muscles to ensure mitochondrial integrity. By evaluating the effects of MCU modulators on mitochondrial calcium, mitochondrial dysfunction, antioxidant capacity, endogenous enzyme activities, and tenderness, we explored the relationship between MCU-mediated mitochondrial calcium homeostasis and tenderness in PM muscles (Fig. 1).

3.1. MCU expression and mitochondrial Ca^{2+} concentration

It has been determined that MCU is the transporter in charge of mitochondrial Ca^{2+} uptake (Baughman et al., 2011). Additionally, MCU was essential for tissue function in both healthy and pathological circumstances as well as mitochondrial energy metabolism (Nemani, Shanmughapriya, & Madesh, 2018). The effect of spermine/Ru360 on

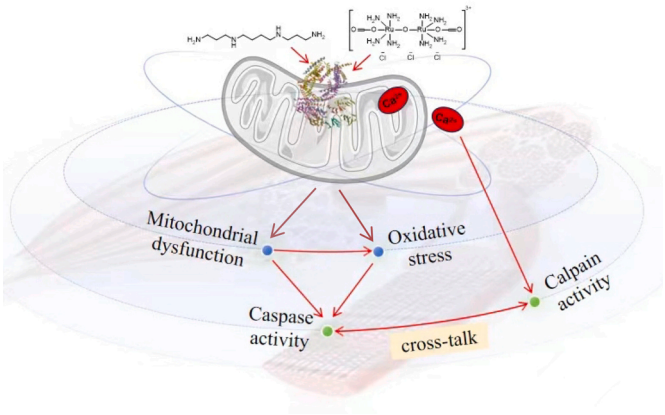

Fig. 1. Experimental design and workflow.

the expression of MCU is shown in Fig. 2A and B. MCU expression increased markedly by extending the duration from 0 h to 24 h in the control group. Compared to the control group at 24 h, the expression levels of MCU were significantly increased and decreased after treatment with spermine and Ru360, respectively. Additionally, mitochondrial Ca^{2+} was examined through mitochondrial isolation to clarify the changes in mitochondrial Ca^{2+} during PM aging, as well as the effect of MCU regulators on mitochondrial calcium homeostasis (Fig. 2C). With the aging time extended, the mitochondrial Ca^{2+} levels in both the control group and the spermine group showed an initial increase followed by a decrease. The mitochondrial Ca^{2+} levels in the spermine group were higher than those in the control group at each corresponding time point and reached a maximum value at 24 h after slaughter. Conversely, the mitochondrial Ca^{2+} levels in the Ru360 group gradually decreased and were lower than those in the control group and the spermine group ($P < 0.05$). Moreover, The impact of the spermine/Ru360 treatment on mitochondrial Ca^{2+} levels was dependent on time (treatment × time, $P < 0.001$). With ATP consumption and pH decline in PM muscles, the calcium uptake capacity of the sarcoplasmic reticulum is disrupted, leading to cytoplasmic calcium overload (Dang, Buhler, Davis, et al., 2020). Mitochondria occupy a noteworthy position in cytoplasmic calcium regulation in skeletal muscle due to the proximity of mitochondria to the sarcoplasmic reticulum and their ability to transport calcium. The aforementioned biochemical process may be the reason for the upregulation of MCU and induction of elevated mitochondrial Ca^{2+} levels at 24 h after slaughter. According to previous findings, spermine and Ru360 could serve as specific activators and inhibitors of MCU, respectively, mediating mitochondrial calcium uptake through upregulation and downregulation of MCU expression (Wu et al., 2021). Similarly, mitochondrial calcium overload resulting from abnormal MCU expression was the main reason for the formation of low-quality chicken breast meat such as wooden breast meat (Zhang, Xing, Li, Zhang, & Gao, 2023). Dang, Buhler, Thornton, Legako, and Matarneh (2020) injected bovine *longissimus thoracis et lumborum* muscle samples with DS16570511, which significantly inhibited mitochondrial calcium uptake and increased free calcium concentration. These results suggested that upregulation of MCU could lead to changes in mitochondrial calcium levels during PM aging, and spermine/Ru360 could be used to construct an MCU-mediated mitochondrial calcium uptake imbalance model.

3.2. MPTP opening and mitochondrial micromorphology

An excessive increase in cytoplasmic calcium resulted in increased mitochondrial calcium uptake, which induced MPTP opening and apoptosis activation (Qi, Li, Jin, Simmen, & Shuai, 2020). Similarly, Wang et al. (2017) utilized the MPTP regulator cyclosporine A to study the effect of MPTP opening mediated by it on the regulation of the

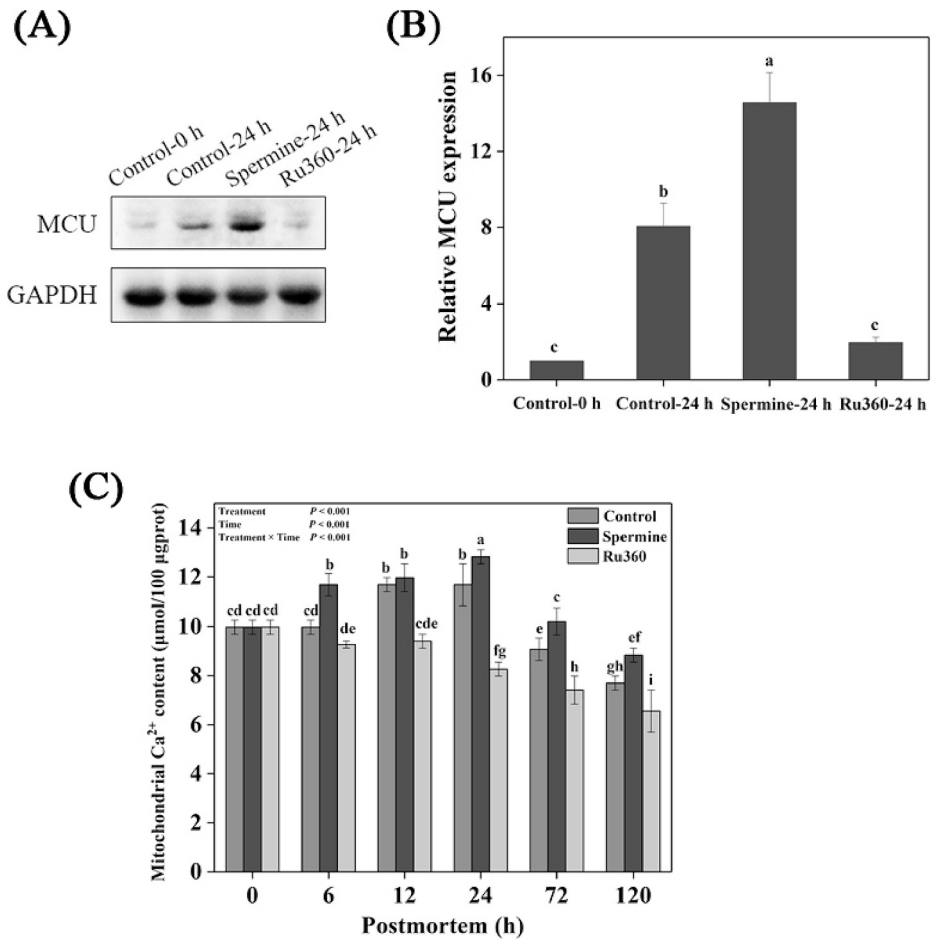

Fig. 2. The effects of spermine and Ru360 on MCU expression and mitochondrial calcium uptake during PM aging. (A) The expression level of MCU in the control group, spermine group, and Ru360 group at 24 h PM. (B) The content of mitochondrial calcium in the three groups during PM aging. Data are presented as mean ± SE. Different letters (a − i) denoted a significant difference ($P < 0.05$). MCU, mitochondrial calcium uniporter, PM, postmortem.

mitochondrial apoptosis pathway in yak meat tenderness and speculated that MPTP opening may be affected by Ca^{2+} overload. It has been shown by Hepple (2016) that MPTP is crucial to the mitochondrial apoptosis pathway. The effect of spermine/Ru360 on the degree of MPTP opening during PM aging of beef meat is shown in Fig. 3A, and the decrease in absorbance reflects an increase in MPTP openness. The MPTP openness of the control group showed a gradually increasing trend ($P < 0.05$), which was in accordance with the report of Wang et al. (2017). There was a significant difference between the spermine group/Ru360 group and the control group from 24 h after slaughter. From 24 h to 120 h, the MPTP opening in Ru360 group was significantly higher than that in the control group ($P < 0.05$), but the MPTP opening in the spermine group was significantly lower than that in the control group ($P < 0.05$) except at 48 h PM. Spermine/Ru360 treatment differentially influenced MPTP over time (treatment × time, $P < 0.001$). The present results were basically consistent with the trend of changes in mitochondrial calcium and demonstrate that the increase in sarcoplasmic calcium led to an increase in mitochondrial calcium uptake, triggering the opening of the MPTP during PM aging, which can be alleviated by the MCU inhibitor.

Additionally, mitochondrial morphology analysis using transmission electron microscopy is shown in Fig. 3B. The mitochondrial structure at 0 h PM was intact, with a smooth outer membrane and a compact cristae structure folded by the inner membrane, similar to physiological mitochondria. The size of mitochondria significantly increased and the outer membrane of mitochondria gradually ruptured, accompanied by some mitochondria exhibiting the vesicular ultrastructure at 24 h PM. In the spermine group, the cristae structure became hazy, and the outer membrane structure of the mitochondria was severely torn at 24 h PM. In contrast, the smoothness of the outer membrane structure and the integrity of the cristae structure in the Ru360 group were better than those in the control group. Analogously, the cristae structure was degraded and discontinuous, and the matrix had a brighter appearance at 24 h and 72 h PM (Li et al., 2020). The above results supported that MCU-mediated mitochondrial calcium homeostasis altered MPTP opening and mitochondrial membrane integrity, which represent mitochondrial function.

3.3. *Oxidative stress and antioxidant capacity*

Excessive activation of MCU can induce an upregulation in mitochondrial Ca^{2+} uptake, often accompanied by an increase in mitochondrial ROS, mediating cell apoptosis (Dong et al., 2017). The overload of mitochondrial Ca^{2+} driven by MCU resulted in mitochondrial dysfunction, inducing more severe mitochondrial ROS overproduction (Liu, et al., 2019). Significant changes in mitochondrial ROS were observed, as shown in Fig. 4A. The amount of mitochondrial ROS fell from 0 to 12 h and rose from 12 to 120 h ($P < 0.05$) in the control group. Previous studies revealed that the ROS level in muscle first decreased and then increased, reaching its lowest point at 6 h or 12 h (Ding et al., 2022; Zhang, Li, Yu, Han, & Ma, 2019). The mitochondrial ROS level at 24 h in *longissimus lumborum* was higher than that at 1 h PM (Zou et al., 2022). The mitochondrial ROS content in the spermine group was significantly higher than that in the control group from 72 to 120 h, while the mitochondrial ROS content in the Ru360 group remained

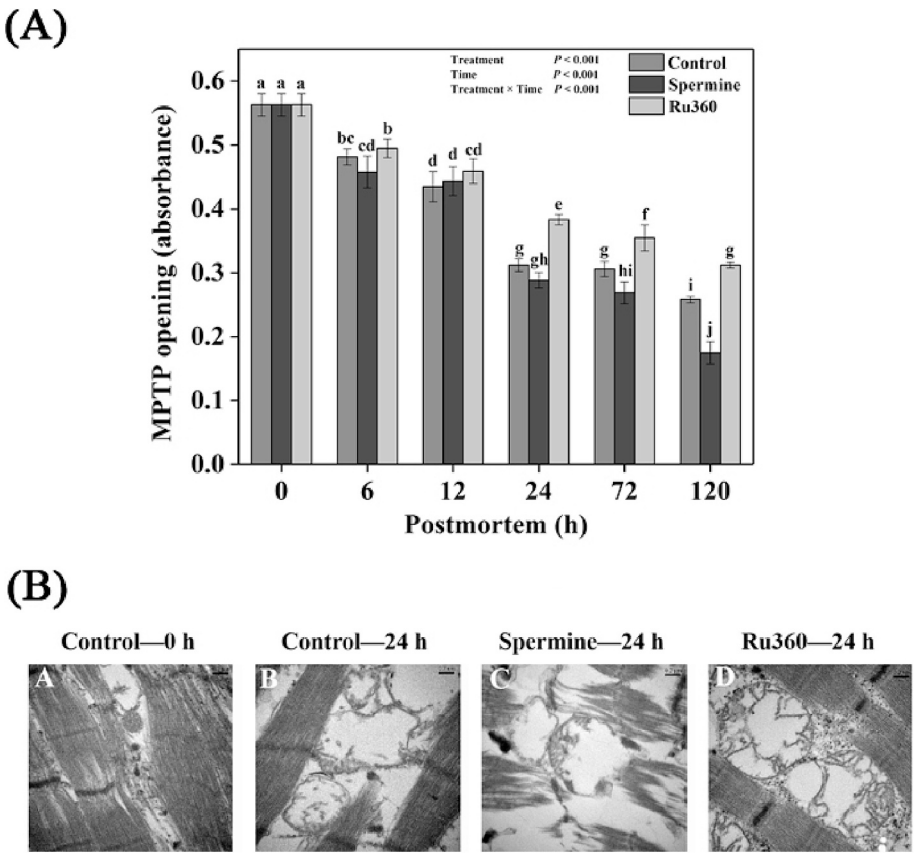

Fig. 3. The effects of spermine and Ru360 on MPTP opening and mitochondrial morphology during PM aging. (A) The changes of MPTP opening in the control group, spermine group, and Ru360 group during PM aging. (B) Mitochondrial morphology in the three groups at 24 h PM (50000×). Data are presented as mean ± SE. Different letters (a − j) denoted a significant difference ($P < 0.05$). MPTP, mitochondrial permeability transition pore, PM, postmortem.

lower than that in the control group from 12 to 120 h PM. Additionally, mitochondrial ROS content was markedly different between the three groups over aging (treatment × time, $P < 0.001$). Spermine and Ru360 could upregulate and downregulate mitochondrial ROS in pathological models, respectively (Liu, et al., 2019; Liu et al., 2020). The intracellular antioxidant system has the effect of clearing ROS content in the early PM period, and oxidative stress can be triggered once the adaptive mechanism of cells to maintain internal balance fails. The initial time of significant differences in mitochondrial ROS induced by spermine and Ru360 compared to the control group was later than the critical time of mitochondrial Ca^{2+}, suggesting that mitochondrial ROS changes may be mediated by mitochondrial Ca^{2+}.

SOD and GSH are key endogenous enzymes that maintain cellular oxidative balance. SOD is a metalloprotein that controls the O^{2-} concentration by catalyzing dismutase, thereby protecting cells from oxidative stress. GSH is a biothiol composed of glutamic acid, cysteine, and glycine, which has the ability to scavenge ROS. SOD and GSH were measured to evaluate the effect of spermine and Ru360 on the antioxidant capacity of muscle cells during PM aging (Fig. 4B, C). The SOD activity in the control group first increased and then decreased and reached a maximum at 72 h. These results were similar to those reported by Wang et al. (2018). The changes in SOD activities in the Ru360 group were consistent with those in the control group and higher than those in the control group from 6 h to 120 h ($P < 0.05$). However, the SOD activity of the spermine group reached its peak earlier than that the control group, and was lower than that of the control group from 12 h to 120 h, except at 24 h. Interestingly, the trend of changes in GSH content and SOD activity in the three groups was basically the same. Spermine/Ru360 treatment influenced GSH content and SOD activity over time (treatment × time, $P < 0.001$). These results were understandable since the activity and content of antioxidant factors were closely related to the degree of intracellular oxidative stress, possibly caused by mitochondrial calcium imbalance.

3.4. Activities of endogenous enzymes

Currently, it has been determined that calpain and caspases are crucial players in the intricate process of myofibrillar protein hydrolysis and are indispensable endogenous enzymes that control PM muscle tenderness (Ding et al., 2021). Calpain is a calcium-dependent cysteine protease distributed on the *Z*-line, and its activity changes are shown in Fig. 5A. In this study, the calpain activity in the control group increased between 0 and 24 h ($P < 0.05$), indicating that the calpain activation was mainly in the early stage of PM aging, and the calpain activity significantly decreased between 24 and 120 h ($P < 0.05$). The calpain activity of the Ru360 group at the corresponding time points was higher than that of the control group and reached its maximum value at 24 h PM, earlier than that of the control group. In contrast, the calpain activity of the spermine group reached its maximum value later than that of the control group. Spermine/Ru360 treatment differentially affected calpain activity over time (treatment × time, $P < 0.001$). Dang, Buhler, Thornton, et al. (2020) found an increase in calpain activity by injecting DS16570511 (an MCU inhibitor), strongly suggesting that it resulted from an increase in free calcium. In other words, the difference in calpain activity between the spermine and Ru360 groups was caused by mitochondrial calcium uptake mediated by MCU regulators, leading to changes in sarcoplasmic calcium.

As mentioned earlier, the mitochondrial pathway is one of the three ways to induce cell apoptosis. The release of apoptotic factors caused by mitochondrial dysfunction, which induced an increase in caspase-9 and

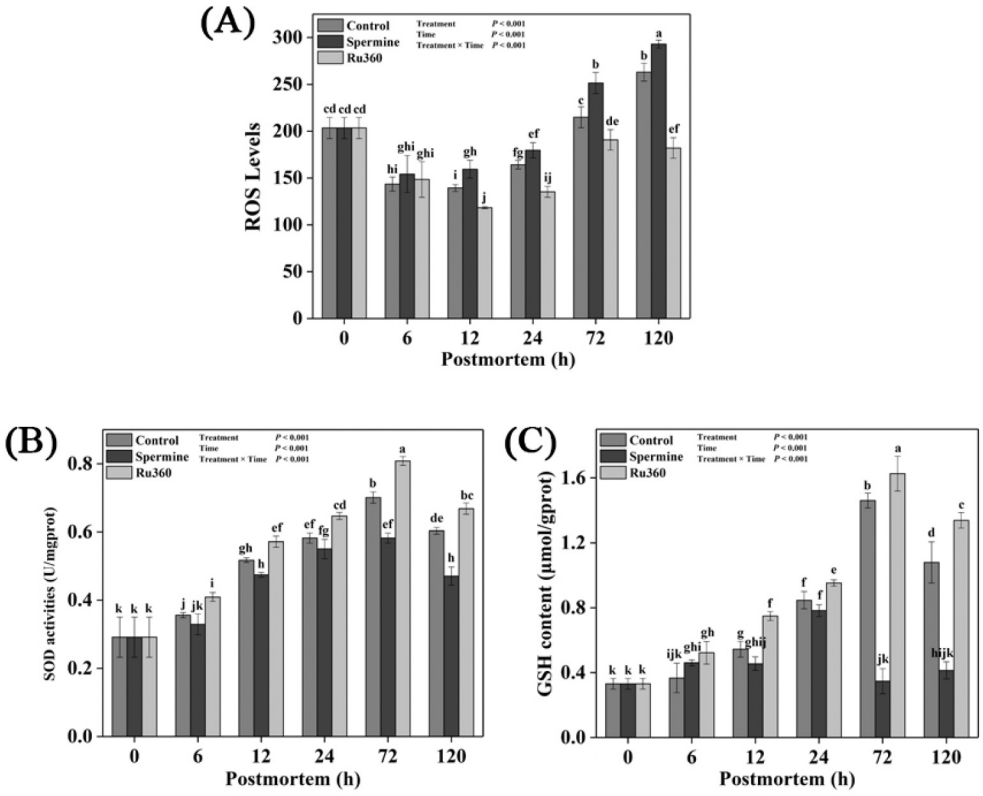

Fig. 4. The effects of spermine and Ru360 on mitochondrial ROS and antioxidant capacity during PM aging. (A) The content of mitochondrial ROS in the control group, spermine group, and Ru360 group during PM aging. (B) The activity of SOD and the content of GSH in the three groups during PM aging. Data are presented as mean ± SE. Different letters (a − k) denoted a significant difference ($P < 0.05$). ROS, reactive oxygen species, SOD, superoxide dismutase, GSH, glutathione, PM, postmortem.

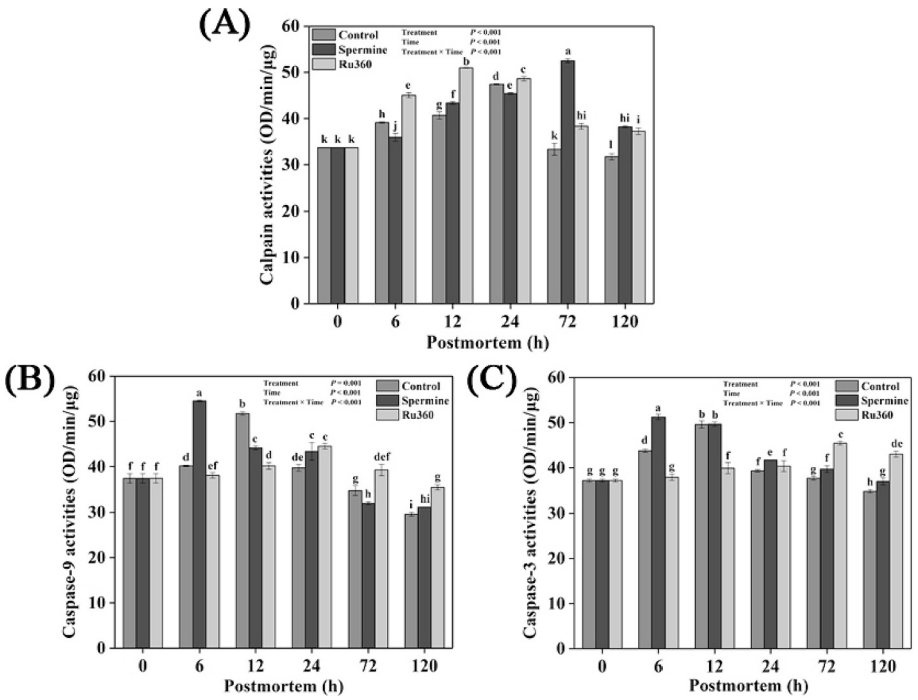

Fig. 5. The effects of spermine and Ru360 on endogenous enzymes activities during PM aging. (A) The changes of calpain activities in the control group, spermine group, and Ru360 group during PM aging. (B) The changes of caspase-9 and caspase-3 activities in the three groups during PM aging. Data are presented as mean ± SE. Different letters (a − l) denoted a significant difference ($P < 0.05$). PM, postmortem.

caspase-3 activities, was a symbol of apoptosis pathway activation and implied that myofibrillar proteins were hydrolyzed by caspases (Zhang et al., 2020). The time when caspase-9 and caspase-3 activities reached their maximum in the three groups was the earliest in the spermine group, followed by the control group, and the latest in the Ru360 group (Fig. 5B, C). Additionally, the caspase-9 and caspase-3 activities of the Ru360 group reached their maximum values at 24 h and 72 h PM, respectively, which is consistent with our previous results (Ding et al., 2022; Wang et al., 2017). The impact of the spermine/Ru360 treatment on caspase-9 and caspase-3 activities was dependent on time (treatment × time, $P < 0.001$). The aforementioned results suggested that there was complex cross-talk between calpain and caspases, which has been partially confirmed by Chen, Feng, Zhang, Xu, and Zhou (2012). Calpastatin serves as an inhibitor of calpain and a substrate of caspase-3, closely linking the two key endogenous enzymes. Notably, calpain not only promoted the formation of MPTP but also directly affected the release of AIF, which could further activate caspases after being released from mitochondria (Kar et al., 2010). Conversely, the Ca^{2+}-ATPase located in the plasma membrane could be cleaved by caspase-3, inactivating the Ca^{2+} pump, and calpain was activated by free calcium (PÁSzty et al., 2007). Thus, MCU-mediated mitochondrial calcium uptake was one of the important influencing factors for the synergistic interaction between calpain and caspases.

3.5. Tenderness of PM beef muscles

MFI reflected I-band breakage and myofibrillar protein hydrolysis, which was a representative indicator for evaluating tenderness PM (Feng et al., 2020). The impact of spermine and Ru360 on MFI is shown in Fig. 6. MFI increased significantly in the three groups over the whole aging stage ($P < 0.05$). The increase in MFI in the control group meant that myofibrillar proteins were gradually broken and degraded during PM aging. The MFI of the spermine group was lower than that of the control group at 6–12 h ($P < 0.05$), and higher than that of the control group at 24–120 h ($P < 0.05$), while the MFI of the Ru360 group was lower than that of the control group throughout the entire aging period ($P < 0.05$). In other words, the spermine group that prioritized mitochondrial dysfunction and induced cell apoptosis had the highest MFI, followed by the control group, and the Ru360 group had the lowest MFI. Moreover, spermine/Ru360 treatment differentially affected MFI over time (treatment × time, $P < 0.001$). It appeared that calpain activation does not play a major role in myofibrillar protein degradation. It was controversial that Dang, Buhler, Davis, et al. (2020) found that the MFI of steaks injected with DS16570511 was higher than that of the control group, indicating a higher degree of proteolysis, and speculated that this may be due to the observation of greater calpain activity in these steaks. The emergence of this contradiction may be due to differences in animal species, resulting in different endogenous enzymes that play a dominant role in myofibrillar protein degradation during PM aging.

4. Conclusions

In summary, this study focused on the effect of mitochondrial calcium uptake on tenderness during PM aging. Spermine and Ru360 were used to construct *in vivo* models that promote and inhibit mitochondrial calcium uptake, respectively. Mitochondrial calcium imbalance induces varying degrees of mitochondrial dysfunction and oxidative stress. These changes triggered the activation of key endogenous enzymes such as calpain and caspase-9/3 at different aging periods, resulting in differences in tenderness between different models. These results demonstrated that MCU-mediated mitochondrial calcium homeostasis plays an indispensable role in the regulation of tenderness and may be the initiator of mitochondrial morphology damage, inducing intracellular redox imbalance and triggering cell apoptosis. This study improved the tenderization mechanism of postmortem meat and laid a theoretical foundation for establishing quality control techniques targeting mitochondria.

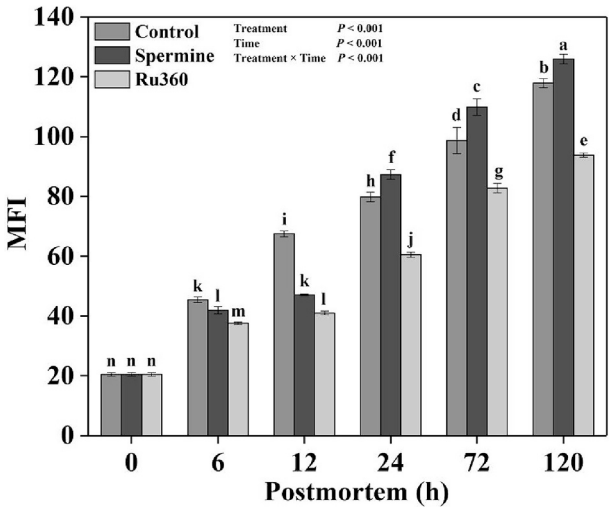

Fig. 6. The changes of MFI in the control group, spermine group, and Ru360 group during PM aging. Data are presented as mean ± SE. Different letters (a – n) denoted a significant difference ($P < 0.05$). MFI, myofibril fragmentation index, PM, postmortem.

CRediT authorship contribution statement

Zhenjiang Ding: Conceptualization, Data curation, Formal analysis, Software, Supervision, Visualization, Writing – original draft, Writing – review & editing. **Chunmei Liu:** Conceptualization, Data curation, Investigation, Methodology, Validation. **Zihan Zhang:** Data curation, Methodology, Resources, Validation, Visualization. **Chunhui Zhang:** Visualization, Writing – review & editing, Funding acquisition, Project administration, Supervision. **Feng Huang:** Data curation, Conceptualization, Funding acquisition, Project administration, Supervision, Visualization, Writing – review & editing.

Declaration of competing interest

The authors declare that they have no known competing financial interests or personal relationships that could have appeared to influence the work reported in this paper.

Data availability

Data will be made available on request.

Acknowledgments

This work was supported by the National Natural Science Foundation of China (Grant Nos: 32072244) and Xinjiang Uygur Autonomous Region Tianshan Talent Training Plan Project (2022TSYCCX0048).

References

Baughman, J. M., Perocchi, F., Girgis, H. S., Plovanich, M., Belcher-Timme, C. A., Sancak, Y., … Mootha, V. K. (2011). Integrative genomics identifies MCU as an essential component of the mitochondrial calcium uniporter. *Nature, 476*(7360), 341–345.

Cao, J., Yu, X., Khan, M. A., Shao, J., Xiang, Y., & Zhou, G. (2012). The effect of calcium chloride injection on shear force and caspase activities in bovine longissimus muscles during postmortem conditioning. *Animal: An International Journal of Animal Bioscience, 6*(6), 1018–1022.

Chen, L., Feng, X. C., Zhang, W. G., Xu, X. L., & Zhou, G. H. (2012). Effects of inhibitors on the synergistic interaction between calpain and caspase-3 during post-mortem aging of chicken meat. *Journal of Agricultural and Food Chemistry, 60*(34), 8465–8472.

Dang, D. S., Buhler, J. F., Davis, H. T., Thornton, K. J., Scheffler, T. L., & Matarneh, S. K. (2020). Inhibition of mitochondrial calcium uniporter enhances postmortem proteolysis and tenderness in beef cattle. *Meat Science, 162*.

Dang, D. S., Buhler, J. F., Thornton, K. J., Legako, J. F., & Matarneh, S. K. (2020). Myosin heavy chain isoform and metabolic profile differ in beef steaks varying in tenderness. *Meat Science, 170*.

Ding, Z., Wei, Q., Liu, C., Zhang, C., & Huang, F. (2022). Comparison of oxidative stress-mitochondria-mediated tenderization in two different bovine muscles during aging. *Food Chemistry: Molecular Sciences, 5*.

Ding, Z., Wei, Q., Zhang, C., Zhang, H., & Huang, F. (2021). Influence of oxidation on heat shock protein 27 translocation, caspase-3 and calpain activities and myofibrils degradation in postmortem beef muscles. *Food Chemistry, 340*.

Dong, Z., Shanmughapriya, S., Tomar, D., Siddiqui, N., Lynch, S., Nemani, N., … Madesh, M. (2017). Mitochondrial Ca^{2+} uniporter is a mitochondrial luminal redox sensor that augments MCU channel activity. *Molecular Cell, 65*(6), 1014–1028.e7.

Feng, Y. H., Zhang, S. S., Sun, B. Z., Xie, P., Wen, K. X., & Xu, C. C. (2020). Changes in physical meat traits, protein solubility, and the microstructure of different beef muscles during post-mortem aging. *Foods, 9*(6).

Green, D. R. (2005). Apoptotic pathways: Ten minutes to dead. *Cell, 121*(5), 671–674.

Guo, B., Zhang, W., Tume, R. K., Hudson, N. J., Huang, F., Yin, Y., & Zhou, G. (2016). Disorder of endoplasmic reticulum calcium channel components is associated with the increased apoptotic potential in pale, soft, exudative pork. *Meat Science, 115*, 34–40.

Hepple, R. T. (2016). Impact of aging on mitochondrial function in cardiac and skeletal muscle. *Free Radical Biology and Medicine, 98*, 177–186.

Huang, F., Huang, M., Zhang, H., Guo, B., Zhang, D., & Zhou, G. (2014). Cleavage of the calpain inhibitor, calpastatin, during postmortem ageing of beef skeletal muscle. *Food Chemistry, 148*, 1–6.

Huang, F., Huang, M., Zhou, G., Xu, X., & Xue, M. (2011). In vitro proteolysis of myofibrillar proteins from beef skeletal muscle by caspase-3 and caspase-6. *Journal of Agricultural and Food Chemistry, 59*(17), 9658–9663.

Jia, S. Z., Xu, X. W., Zhang, Z. H., Chen, C., Chen, Y. B., Huang, S. L., … Song, G. L. (2021). Selenoprotein K deficiency-induced apoptosis: A role for calpain and the ERS pathway. *Redox Biology, 47*.

Kar, P., Samanta, K., Shaikh, S., Chowdhury, A., Chakraborti, T., & Chakraborti, S. (2010). Mitochondrial calpain system: An overview. *Archives of Biochemistry and Biophysics, 495*(1), 1–7.

Kiyimba, F., Hartson, S. D., Rogers, J., VanOverbeke, D. L., Mafi, G. G., & Ramanathan, R. (2022). Dark-cutting beef mitochondrial proteomic signatures reveal increased biogenesis proteins and bioenergetics capabilities. *Journal of Proteomics, 265*.

Li, X., Zhang, D., Ijaz, M., Tian, G., Chen, J., & Du, M. (2020). Colour characteristics of beef longissimus thoracis during early 72 h postmortem. *Meat Science, 170*.

Liu, C., Ding, Z., Zhang, Z., Zhao, L., Zhang, C., & Huang, F. (2023). Morphological changes of mitochondria-related to apoptosis during postmortem aging of beef muscles. *Food Chemistry, X*, 19.

Liu, Y., Jin, M., Wang, Y., Zhu, J., Tan, R., Zhao, J., Ji, X., Jin, C., Jia, Y., Ren, T., & Xing, J. (2020). MCU-induced mitochondrial calcium uptake promotes mitochondrial biogenesis and colorectal cancer growth. *Signal Transduction and Targeted Therapy, 5*(1).

Liu, Z., Zhao, W., Yuan, P., Zhu, P., Fan, K., Xia, Z., & Xu, S. (2020). The mechanism of CaMK2α-MCU-mitochondrial oxidative stress in bupivacaine-induced neurotoxicity. *Free Radical Biology and Medicine, 152*, 363–374.

Ma, G., Zhang, J., Wang, Z., Yu, Q., & Han, L. (2023). Effects of muscle-specific oxidative stress on protein phosphorylation and its relationship with mitochondrial dysfunction, muscle oxidation, and apoptosis. *Food Chemistry, 427*.

Nemani, N., Shanmughapriya, S., & Madesh, M. (2018). Molecular regulation of MCU: Implications in physiology and disease. *Cell Calcium, 74*, 86–93.

Olson, D. G., Parrish, J. R., & Stromer, M. H. (1976). Myofibril fragmentation and shear resistance of three bovine muscles during postmortem storage. *Journal of Food Science, 41*, 1036–1041.

PÁSzty, K., Antalffy, G., HegedÜS, L., PadÁNyi, R., Penheiter, A. R., Filoteo, A. G., … Enyedi, Á. (2007). Cleavage of the plasma membrane Ca+aTPase during apoptosis. *Annals of the New York Academy of Sciences, 1099*(1), 440–450.

Qi, H., Li, X., Jin, Z., Simmen, T., & Shuai, J. (2020). The oscillation amplitude, not the frequency of cytosolic calcium, regulates apoptosis induction. *iScience, 23*(11).

Qiu, Y., Cheng, R., Liang, C., Yao, Y., Zhang, W., Zhang, J., Zhang, M., Li, B., Xu, C., & Zhang, R. (2020). MicroRNA-20b promotes cardiac hypertrophy by the inhibition of mitofusin 2-mediated inter-organelle Ca^{2+} cross-talk. *Molecular Therapy - Nucleic Acids, 19*, 1343–1356.

Scheffler, T. L., & Gerrard, D. E. (2007). Mechanisms controlling pork quality development: The biochemistry controlling postmortem energy metabolism. *Meat Science, 77*(1), 7–16.

Sun, C., Zhu, L., Qin, H., Su, H., Zhang, J., Wang, S., Xu, X., Zhao, Z., Mao, G., & Chen, J. (2023). Inhibition of mitochondrial calcium uptake by Ru360 enhances the effect of 1800 MHz radio-frequency electromagnetic fields on DNA damage. *Ecotoxicology and Environmental Safety, 264*.

Wang, L. L., Du, R. S., Li, J., Cai, Z. J., Han, L., Mao, Y., … Chen, L. H. (2021). The potential mediation of nitric oxide in the activation of mitochondrion-dependent apoptosis and yak meat tenderness during postmortem aging. *Food Bioscience, 42*.

Wang, L. L., Han, L., Ma, X. L., Yu, Q. L., & Zhao, S. N. (2017). Effect of mitochondrial apoptotic activation through the mitochondrial membrane permeability transition pore on yak meat tenderness during postmortem aging. *Food Chemistry, 234*, 323–331.

Wang, L. L., Yu, Q. L., Han, L., Ma, X. L., Song, R. D., Zhao, S. N., & Zhang, W. H. (2018). Study on the effect of reactive oxygen species-mediated oxidative stress on the activation of mitochondrial apoptosis and the tenderness of yak meat. *Food Chemistry, 244*, 394–402.

Wang, T., Feng, X., Li, L., Luo, J., Liu, X., Zheng, J., Fan, X., Liu, Y., Xu, X., Zhou, G., & Chen, L. (2022). Effects of quercetin on tenderness, apoptotic and autophagy signalling in chickens during post-mortem ageing. *Food Chemistry, 383*.

Weiser, A., Hermant, A., Bermont, F., Sizzano, F., Karaz, S., Alvarez-Illera, P., … De Marchi, U. (2023). The mitochondrial calcium uniporter (MCU) activates mitochondrial respiration and enhances mobility by regulating mitochondrial redox state. *Redox Biology, 64*.

Wu, R., Zuo, W., Xu, X., Bi, L., Zhang, C., Chen, H., Liu, H., & Xu, Z. (2021). MCU that is transcriptionally regulated by Nrf2 augments malignant biological behaviors in oral squamous cell carcinoma cells. *BioMed Research International, 2021*, 1–17.

Zhang, J., Li, M., Yu, Q., Han, L., & Ma, Z. (2019). Effects of lysosomal–mitochondrial apoptotic pathway on tenderness in post-mortem bovine longissimus muscle. *Journal of Agricultural and Food Chemistry, 67*(16), 4578–4587.

Zhang, J., Ma, D., & Kim, Y. H. B. (2020). Mitochondrial apoptosis and proteolytic changes of myofibrillar proteins in two different pork muscles during aging. *Food Chemistry, 319*.

Zhang, X., Xing, T., Li, J., Zhang, L., & Gao, F. (2023). Mitochondrial dysfunction and calcium dyshomeostasis in the pectoralis major muscle of broiler chickens with wooden breast myopathy. *Poultry Science, 102*(9).

Zou, B., Jia, F., Ji, L., Li, X., & Dai, R. (2023). Effects of mitochondria on postmortem meat quality: Characteristic, isolation, energy metabolism, apoptosis and oxygen consumption. *Critical Reviews in Food Science and Nutrition*, 1–24.

Zou, B., Yu, Q., Shao, L., Sun, Y., & Li, X. (2022). Dai, R., alteration of mitochondrial lipidome and its potential effect on apoptosis, mitochondrial reactive oxygen species production, and muscle oxidation in beef during early postmortem. *Journal of Agricultural and Food Chemistry, 70*(26), 8064–8074.